

# Quantum Degenerate Exciton-Polaritons in Thermal Equilibrium

Hui Deng, David Press, and Stephan Gotzinger

Quantum Entanglement Project, ICORP,

JST, Edward L. Ginzton Laboratory,

Stanford University, Stanford, California 94305, USA

Jeffrey S. Solomon

Edward L. Ginzton Laboratory, Stanford University, Stanford CA 94035, USA

Rudolf Hey and Klaus H. Ploog

Paul-Drude-Institut für Festkörperelektronik,

Hausvogteiplatz 5-7, D-10117 Berlin, Germany

Yoshihisa Yamamoto

Quantum Entanglement Project, ICORP, JST,

Edward L. Ginzton Laboratory, Stanford University,

Stanford, California 94305, USA and

National Institute of Informatics, Tokyo, Japan

## Abstract

We study the momentum distribution and relaxation dynamics of semiconductor microcavity polaritons by angle-resolved and time-resolved spectroscopy. Above a critical pump level, the thermalization time of polaritons at positive detunings becomes shorter than their lifetime, and the polaritons form a quantum degenerate Bose-Einstein distribution in thermal equilibrium with the lattice.

Quantum phase transitions provide a key to the understanding of many-body quantum physics such as Bose-Einstein Condensation, superuidity, and superconductivity. Complementary to cold atomic gases, excitons (bound electron-hole pairs) and polaritons (strongly coupled excitons and photons) have emerged as unique solid-state systems for studying collective quantum phenomena. A variety of quantum phases are predicted for excitons and polaritons, including BEC, superuidity, and crossover from BEC to Bardeen-Cooper-Schrieffer states[1, 2, 3, 4, 5, 6, 7, 8]. Most notably, polaritons have an effective mass and energy density of states eight orders of magnitude smaller than those of hydrogen atoms, and four orders of magnitude smaller than those of excitons. Hence the critical temperatures of phase transitions for polaritons range from 1K up to room temperature. Moreover, at a given temperature, the quantum degeneracy condition for polaritons is fulfilled at a density eight orders of magnitude lower than that required for atoms. Stimulated scattering and lasing of polaritons have been observed by many groups[9, 10, 11, 12, 13, 14, 15]. However, the polariton gases in these experiments were far from equilibrium.

Polaritons are elementary excitations of semiconductors with relatively short lifetimes, thus it is generally difficult to cool hot polaritons to the lattice temperature before they decay. On the lower energy branch, polaritons change from exciton-like lower polaritons (ELPs) at large inplane wavenumber  $k$  to half-exciton half-photon lower polaritons (LPs) at  $k = 0$ . Correspondingly, their lifetime decreases by two orders of magnitude and their energy density of states decreases by four orders of magnitude. Hence an energy relaxation bottleneck is commonly observed [12, 16, 17, 18] at low densities where spontaneous linear phonon-LP scattering is the dominant, yet insufficient, cooling mechanism. When the quantum degeneracy condition of  $N_{LP} \gg 1$  is fulfilled, bosonic stimulated stimulation greatly enhances both the nonlinear LP-LP scattering and the linear LP-phonon scattering [9, 10, 11, 12, 15]. Recently, a degenerate Bose-Einstein distribution (BED) of LPs has been observed [19, 20], but the LP temperature was  $T_{LP} \approx 100$  K, much higher than the lattice temperature  $T_{lat} \approx 4.2$  K. This suggests that although LP-LP scattering establishes quasi-equilibrium among LPs, cooling by the phonon bath is still slower than the decay of the LPs.

Fortunately the lifetime and thermalization time of the polaritons can be controlled by adjusting the detuning of photon energy relative to the exciton energy at  $k = 0$ . With increasing positive  $\delta$ , the excitonic fraction of a LP  $\frac{N_{exc}}{N_{LP}} = \frac{4}{(\frac{\omega_{ph}}{\omega_{exc}})^2 + 4}$  increases, while the energy density of states  $(E) / (1 + \frac{4}{(\frac{\omega_{ph}}{\omega_{exc}})^2})^{\frac{1}{2}}$  also increases (where  $\omega_{exc}$  is the upper-

lower polariton splitting). Hence the LP lifetime  $\tau_{LP, cav} = (1/\Gamma_{exc})$  becomes longer, and LP-phonon scattering rates ( $\Gamma_{exc}/E$ ) and LP-LP scattering rates ( $\Gamma_{exc}^2/E$ ) become larger. At very large positive detunings, the observation of cooperative effects is eventually prohibited by the higher critical density, stronger exciton localization, and shorter dephasing time of ELPs. In this paper, we report the observation of a quantum degenerate polariton gas in thermal equilibrium with the lattice at moderate positive detunings. This is confirmed by measurement of both the LP's thermalization time vs. lifetime, and time-resolved momentum distributions of the LPs.

The MBE-grown sample studied in this paper consists of a  $\approx 2$   $\mu\text{m}$  cavity sandwiched between  $\text{Ga}_{0.865}\text{Al}_{0.135}\text{As}/\text{AlAs}$  distributed Bragg reflectors. Three stacks of QW are placed at the central three antinodes of the microcavity, each stack consisting of four 6.8 nm-thick  $\text{GaAs}$  QWs separated by 2.7 nm-thick  $\text{AlAs}$  layers. The microcavity thickness is tapered to allow tuning of the cavity resonance from the center to the edge of the sample. We focus a linearly polarized picosecond mode-locked Ti-Sapphire laser onto a 50  $\mu\text{m}$ -diameter spot on the sample. The LP population per mode  $N_{LP}(k)$  is measured directly by angle-resolved photon-ux since there exists a one-to-one correspondence between the two via the  $k$ -dependent lifetime of the LPs. At an incidence angle of 50° from the sample growth direction, the laser resonantly pumps the corresponding ELP modes. The emitted light is collected with an angular resolution of 0.5° in air by an optical fiber which is in turn connected to an imaging spectrometer and/or a streak camera with a time resolution of 4 ps. Details of the experimental setup can be found in Ref [19].

In all experiments, we attach the sample to a copper coldfinger kept at 4.2 K. Reflection and dispersion measurements show that the uncoupled exciton resonance is 1.597 eV, and the splitting between upper and lower polariton is  $\approx 14.4$  meV at zero detuning. We measured the LP emission intensity at  $k = 0$  vs. pump power  $P$  and observed a quantum degeneracy threshold for detunings between  $-5$  meV and  $+10$  meV (Fig. 1 (a)). When the estimated LP number per pulse  $I_{LP}(k = 0) \approx 121$ ,  $I_{LP}$  starts to increase nonlinearly with  $P$ , indicating the onset of stimulated scattering into the state. We define the operational threshold  $P_{th}$  at the steepest slope of the input-output curve.  $P_{th}$  ranges from 5 to 20 mW, corresponding to injected ELP densities  $n_{QW} \approx 1.5 \times 10^{10} \text{ cm}^{-2}$  per QW. At the highest pump power of  $P_{max} = 100$  mW,  $n_{QW} \approx 2.5 \times 10^{10} \text{ cm}^{-2}$  per QW. The observed mean-field blueshift of the LP energy  $E_{LP}(k = 0)$  is less than 1 meV for all detunings and pump

powers. At  $\Delta = 6.7$  meV,  $E_{LP}(k=0)$  is 0.2 to 0.3 meV from  $P_{th}$  to  $P_{max}$ . Energy and momentum dispersion relations below and above threshold are measured to further confirm that the system stays in the strong coupling regime.

A prerequisite for reaching thermal equilibrium is that the LP's thermalization time must be faster than their lifetime. Shown in Fig. 1 (b) is the time evolution of  $N_{LP}(k=0)$ . To estimate the LP energy thermalization time vs. lifetime, we model the system with two coupled modes, the  $k=0$  LP ground state and the hot ELP reservoir:

$$\begin{aligned}\frac{\partial N_R}{\partial t} &= P(t) \frac{N_R}{\tau_R} - \frac{N_R}{\tau_{therm}} \\ \frac{\partial N_0}{\partial t} &= \frac{N_0}{\tau_0} + \frac{N_R}{\tau_{therm}};\end{aligned}\quad (1)$$

where  $N_R$  and  $N_0$  are the ELP reservoir and LP ground state populations, respectively.  $P(t)$  is an external pump represented by a Gaussian pulse, centered at  $t=0$  with a pulse width of 3 ps.  $\tau_{therm}$  is the thermalization time from ELPs to the LP ground state.  $\tau_R$  and  $\tau_0$  are the lifetime of the ELPs and LP ground state, respectively.  $\tau_0$  can be determined from the cavity lifetime of  $\tau_{cav} = 2$  ps and the detuning-dependent photon fraction  $\eta_{cav}$  of the LP ground state:  $\tau_0 = \tau_{cav} = \tau_{cav}$ . We use the normalized  $N_0(t)$  to fit the experimental curve.  $\tau_R$  much longer than  $\tau_0$  and  $\tau_{therm}$ , it has little influence on the fitting, so we set  $\tau_R$  to infinity.  $\tau_{therm}$  is the single fitting parameter. Despite the simplicity of the model, good agreement between data and the fitting curve is obtained as shown in Fig. 1 (b).

In Fig. 1 (c), we plot the normalized thermalization time  $\tau_{therm} = \tau_0$ . For all detunings there is a steep decrease of  $\tau_{therm}$  near the quantum degeneracy threshold, reflecting the onset of stimulated scattering into the LP ground state. At a positive detuning of  $\Delta = 6.7$  meV,  $\tau_{therm}$  shortens from more than 20  $\tau_0$  below threshold to around  $\tau_0$  near threshold, and saturates at about 0.1  $\tau_0$  well above threshold. We expect that thermal equilibrium with the phonon bath may therefore be established above threshold with a quantum degenerate LP population in the ground state. For negative detunings,  $\tau_{therm} = \tau_0$  saturates above unity and the system is expected to stay in a non-equilibrium condition.

We then measure the time-resolved LP momentum distribution  $N_{LP}(t; k)$  [21] and compare it to the classical Maxwell-Boltzmann distribution (MBD)  $N_{MB}(k)$  and the quantum mechanical Bose-Einstein distribution  $N_{BE}(k)$ . Referencing the LP band bottom as energy

zero, we have:

$$\begin{aligned} N_{MB}(k) &= N_0 \exp\left(-\frac{E_{LP}(k)}{k_B T_{LP}}\right); \\ N_{BE}(k) &= 1 - \left[\exp\left(-\frac{E_{LP}(k)}{k_B T_{LP}}\right) (1 + N_0^{-1}) - 1\right]; \end{aligned} \quad (2)$$

The fitting parameters are the LP temperatures  $T_{LP}$ , and the LP population  $N_0$  at  $k = 0$ . The normalized chemical potential is defined by:

$$\mu = -k_B T_{LP} = \ln(1 + N_0^{-1}); \quad (3)$$

At positive detunings  $> 1 \text{ m eV}$ , no bottleneck is observed at any pump level. Above threshold, about 30 ps after the pump pulse, the experimental data are very well described by a BED (except for some extra population at  $k = 0$ ), but not at all by a MBD, as shown in Fig. 2 (a). From BED fitting, we obtain a  $T_{LP}$  close to the lattice temperature  $T_{lat}$ , and a normalized chemical potential  $= 0.01 \pm 0.05$ . Note that quantum degeneracy threshold  $N_0 = 1$  is reached at  $\mu = \ln 2 = 0.7$ . The results indicate that LPs are well thermalized with the phonon bath, forming a quantum degenerate Bose-Einstein distribution at the lattice temperature. This is consistent with the observation that  $N_0$  at positive detunings above threshold.

At small detunings  $|\mu| < 1 \text{ m eV}$ , although a bottleneck exists at most pump levels, quantum degeneracy threshold is still achieved at  $k = 0$ . The momentum distribution in the region  $|\mu| < 0.4 \text{ m eV}$  agrees well with BED (Fig. 2 (b)). However, the fitted  $T_{LP}$  is larger than  $3T_{lat}$ . This suggests that LPs with small  $k$  can temporarily reach quasi-equilibrium among themselves via efficient LP-LP scattering, yet decay out of the system before they can be sufficiently cooled by phonon emission. At large negative detunings  $< -1 \text{ m eV}$ , a strong bottleneck prevents the system from reaching thermal equilibrium (Fig. 2 (c)).

In Fig. 3 we plot the time evolution of the fitted LP temperature  $T_{LP}$  and normalized chemical potential. At 30–40 ps after the pump pulse injects hot LPs, phonon-scattering cools the system to a lowest temperature of  $T_{min} = T_{lat}$  for  $\mu = 6.7 \text{ and } 9.0 \text{ m eV}$ , with a fitted chemical potential  $= 0.1$ . The quantum degenerate LP gas remains in thermal equilibrium at  $T_{lat}$  for a duration of about 20 ps. At the tail of the pulse, the LP population largely decays out of the system,  $N_0$  increases to about  $k_B T_{LP}$  and stimulated scattering diminishes. Since LPs at small  $k$  decay faster than those at larger  $k$ , the temperature of the system starts to rise. The smallest chemical potential  $= 3 \times 10^{-3} \pm 10^{-1}$  is found at

10 | 20 ps after the pump pulse when  $N_{LP}(t)$  is at its peak. For smaller detunings,  $T_{min}$  is higher than  $T_{lat}$ , so thermal equilibrium is not reached.

We choose a time 5 | 10 ps after the LP temperature reaches  $T_{min}$ , when the BED agrees very well with the data, and plot the pump power dependence of  $T_{LP}$  and  $\tau_{therm}$  in Fig. 4. As shown in Fig. 4 (b), decreases with increasing pump level, crossing the quantum degeneracy threshold  $= 0.7$  at  $P = P_{th}$ . This is because the stimulated scattering into the LP ground state becomes prominent when the quantum degeneracy of LPs is established. In Fig. 4 (a),  $T_{LP}$  drops to a minimum value at  $P = 2 | 4P_{th}$ . At approximately the same pump level, the thermalization time  $\tau_{therm}$  reaches its minimum (Fig. 1 (c)). At high pump levels, we notice that  $T_{LP}$  increases, possibly because  $T_{lat}$  increases due to insufficient heat dissipation of the sample to the copper cold finger.

In summary, we found that the dynamical evolution of the momentum distribution of LPs strongly depends on the detuning. At positive detunings, and at pump levels above the quantum degeneracy threshold, LPs establish thermal equilibrium with the phonon bath for a period of about 20 ps, with a chemical potential  $\epsilon_{LP}$  of about  $0.1k_B T$ . The thermalization time  $\tau_{therm}$  of the system is one tenth of the lifetime  $\tau_{LP}(0)$  of the LP ground state. Near resonance ( $|j| < 1 \text{ meV}$ ),  $\tau_{therm}$  becomes comparable to  $\tau_{LP}(0)$ . Stimulated LP-LP scattering is still effective to achieve a quasi-equilibrium BED among LPs in  $k < 1 \text{ m}^{-1}$  at a temperature  $T_{LP}$  significantly higher than the lattice temperature  $T_{lat}$  with a chemical potential  $\epsilon_{LP} = 0.01$  to  $0.1k_B T$ . At large negative detunings,  $\tau_{therm}$  is longer than  $\tau_{LP}(0)$ , so the system never reaches equilibrium.

---

[1] L. Keldysh and A. N. Kozlov, Sov. Phys. JETP 27, 521 (1968).

[2] C. Comte and P. Nozieres, J. Phys. 43, 1069 (1982).

[3] P. Littlewood, P. Eastham, J. Keeling, F. M. Marchetti, and M. Szymanska, J. Phys.: Cond. Matt. 16, S3597 (2004), and references therein.

[4] G. Malpuech, Y. Rubo, F. Laussy, P. Bignonwald, and A. Kavokin, Semicond. Sci. Technol. 18, S395 (2003).

[5] D. Sarchi and V. Savona, arXiv.org:cond-mat/0411084 and 0603106 (2006).

[6] D. Snoke, S. Denev, Y. Liu, L. Pfeifer, and K. West, Nature 418, 754 (2002).

[7] L.V. Butov, A.C. Gossard, and D.S. Chemla, *Nature* 418, 751 (2002).

[8] C.W. Lai, J. Zoch, A.C. Gossard, and D.S. Chemla, *Science* 303, 503 (2004).

[9] L.S. Dang, D. Heger, R. Andre, F. Boeuf, and R. Romestain, *Phys. Rev. Lett.* 81, 3920 (1998).

[10] P. Senellart and J. Bloch, *Phys. Rev. Lett.* 82, 1233 (1999).

[11] P.G. Savvidis, J.J. Baumberg, R.M. Stevenson, M.S. Skolnick, D.M.W. Hattaker, and J.S. Roberts, *Phys. Rev. Lett.* 84, 1547 (2000).

[12] R. Huang, Y. Yamamoto, R. Andre, J. Blaese, M. Muller, and H. Ummer-Tuogo, *Phys. Rev. B* 65, 165314 (2002).

[13] H. Deng, G. Weihs, C. Santori, J. Bloch, and Y. Yamamoto, *Science* 298, 199 (2002).

[14] M. Richard, J. Kasprzak, R. Romestain, R. Andre, and L.S. Dang, *Phys. Rev. Lett.* 94, 187401 (2005).

[15] J. Bloch, B. Semage, M. Perrin, P. Senellart, R. Andre, and L.S. Dang, *Phys. Rev. B* 71, 155311 (2005).

[16] F. Tassone, C. Piermarocchi, V. Savona, and A. Quattropani, *Phys. Rev. B* 56, 7554 (1997).

[17] M. Muller, J. Blaese, R. Andre, and H. Ummer-Tuogo, *Physica B* 272, 476 (1999).

[18] A. Tartakovskii, M. Eman-Ismail, R. Stevenson, M. Skolnick, V. A stratov, D.M.W. Hattaker, J. Baumberg, and J. Roberts, *Phys. Rev. B* 62, R2283 (2000).

[19] H. Deng, G. Weihs, D. Snoke, J. Bloch, and Y. Yamamoto, *Proc. Natl. Acad. Sci.* 100, 15318 (2003).

[20] T.D. Doan, H.T. Cao, D.T. Thoai, and H. H aug, *Phys. Rev. B* 72, 85301 (2005).

[21] The instantaneous LP number density  $N_{LP}(k; t)$  is converted from the count rate  $N_c(k; t)$  according to:  $N_c(k; t) = f_p N_{LP}(k; t) M(k)$ , where  $\Omega(k)$  is the far field emission angle of LPs.  $\Omega(k)$  is the radiative lifetime of the LPs.  $M(k)$  is the number of transverse states at  $k$  subtended by the acceptance angle of the detector.  $f_p = 0.01$ .  $f_p = 78$  MHz is the repetition rate of the pumping laser.  $f_p$  is the overall collection efficiency. Similarly, the time integrated LP number per pulse  $I_{LP}(k = 0)$  is converted from the count rate  $I_c(k = 0) = f_p I_{LP}(k = 0)$ .  $f_p$  and  $I_c(k = 0)$  are calibrated by replacing the sample by a fiber tip and sending a few milliwatts of light through the fiber.

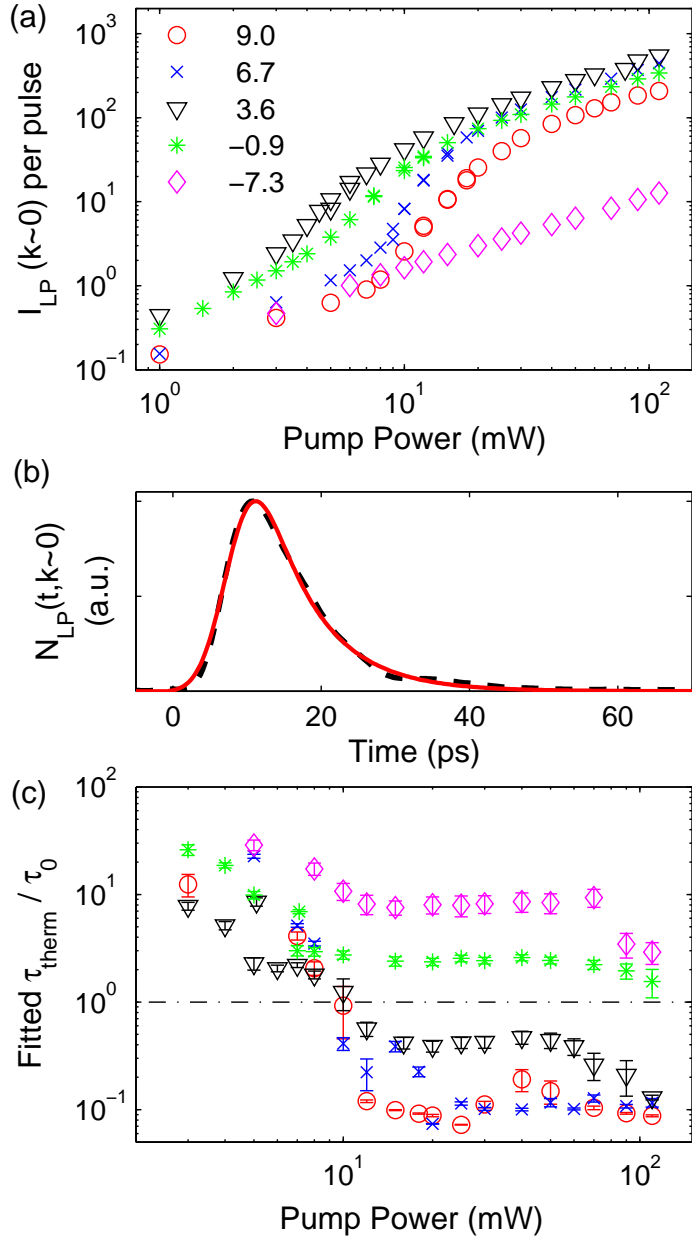


FIG. 1: (a) LP number per pulse  $I_{LP}(k \sim 0)$  [21] vs. pump power at different detunings. No threshold is observed for  $\Delta = -7.3$  m eV. (b) Time evolution of ground state LP emission intensity  $N_{LP}(t, k \sim 0)$ . The dashed line is data taken for  $\Delta = 6.7$  m eV,  $P = 20$  mW, deconvolved with the streak camera resolution of 4 ps. The solid line is a fit to Eq. (1). (c) Normalized thermalization time  $\tau_{\text{therm}} / \tau_0$  vs. pump power at different detunings. Below the dash-dotted line,  $\tau_{\text{therm}}$  becomes shorter than  $\tau_0$ , so thermal equilibrium is expected. Detunings in m eV are given in the figure legend.

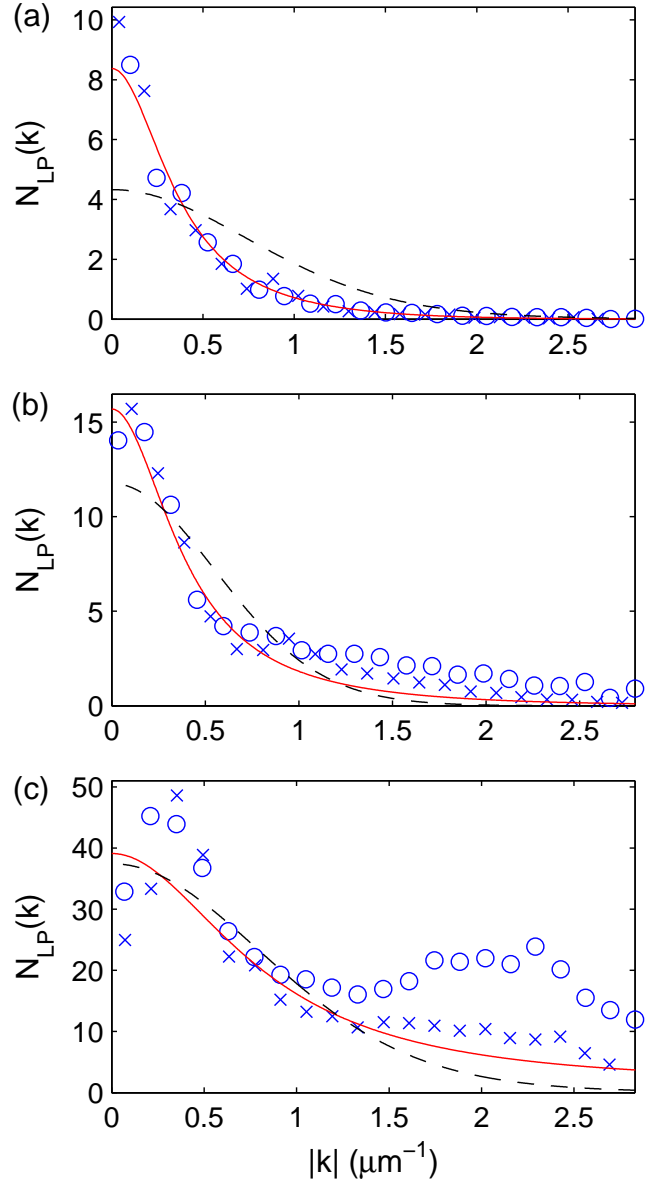


FIG. 2: LP number per state  $N(t; k)$  vs. in-plane wavenumber  $|k|$  for different detunings at a time when  $T_{LP}$  reaches  $T_{m\text{ in}}$ : (a)  $\Delta = 6.7 \text{ meV}$ ,  $P = 4P_{\text{th}}$ ; (b)  $\Delta = 0.9 \text{ meV}$ ,  $P = 4P_{\text{th}}$ ; (c)  $\Delta = 3.85 \text{ meV}$ ,  $P = 6P_{\text{th}}$ . Crosses are data taken from the incidence direction of the pump, open circles are from the reaction direction, solid lines are fitting by BED, and dashed lines by MBD. Parameters for the curves are: (a)  $T_{MB} = 4 \text{ K}$ ,  $T_{BE} = 4.4 \text{ K}$ ,  $\gamma_{BE} = 0.04 \text{ meV}$ ; (b)  $T_{MB} = 4 \text{ K}$ ,  $T_{BE} = 8.1 \text{ K}$ ,  $\gamma_{BE} = 0.13 \text{ meV}$ ; (c)  $T_{MB} = 8.5 \text{ K}$ ,  $T_{BE} = 182 \text{ K}$ ,  $\gamma_{BE} = 0.4 \text{ meV}$ .

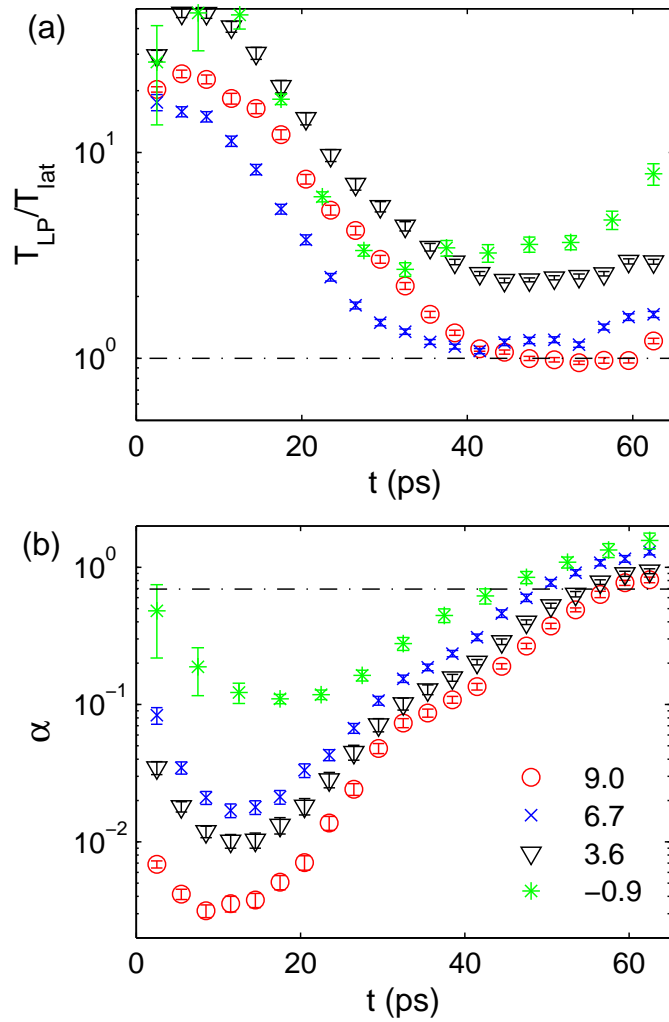


FIG. 3: Time evolution of (a) normalized LP temperature  $T_{LP}/T_{lat}$  and (b) normalized chemical potential  $\alpha = -k_B T_{LP}/T$ , obtained from BED fitting of the LP momentum distribution, at  $T_{lat} = 42$  K and  $P = 3P_{th}$ .  $\alpha$  in meV is given in the legend.

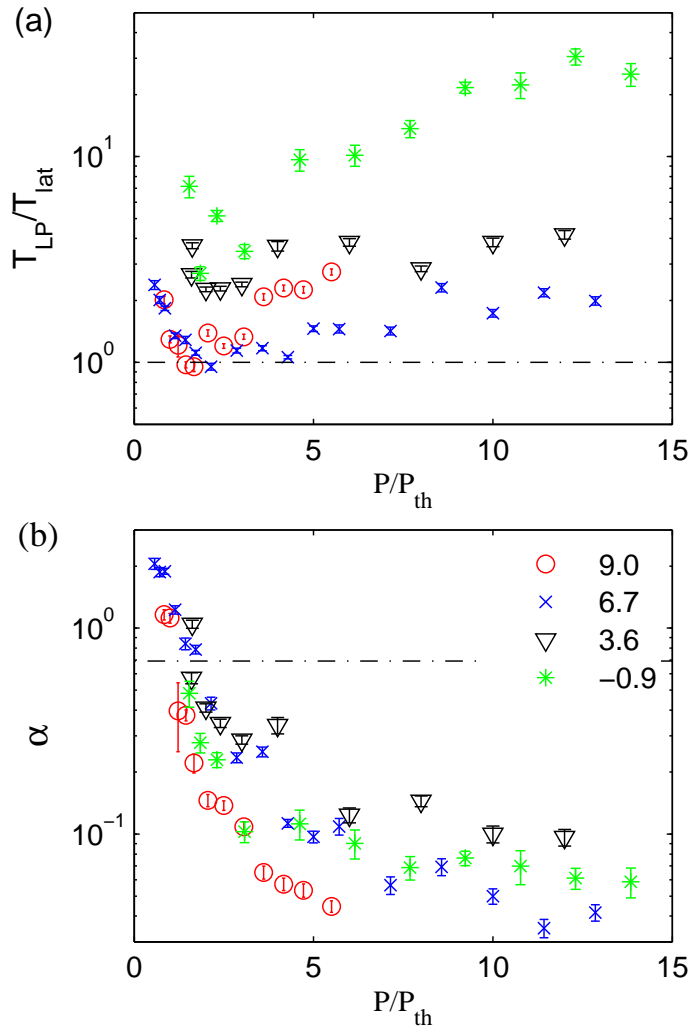


FIG. 4: Pump dependence of (a)  $T_{LP}/T_{lat}$  and (b)  $\alpha = -k_B T$ , obtained from BED fitting of the LP momentum distribution. Time  $t$  is chosen as when  $T_{LP}$  is at its minimum.  $T_{lat} = 42$  K,  $P = 3P_{th}$ .  $\alpha$  in meV is given in the legend.

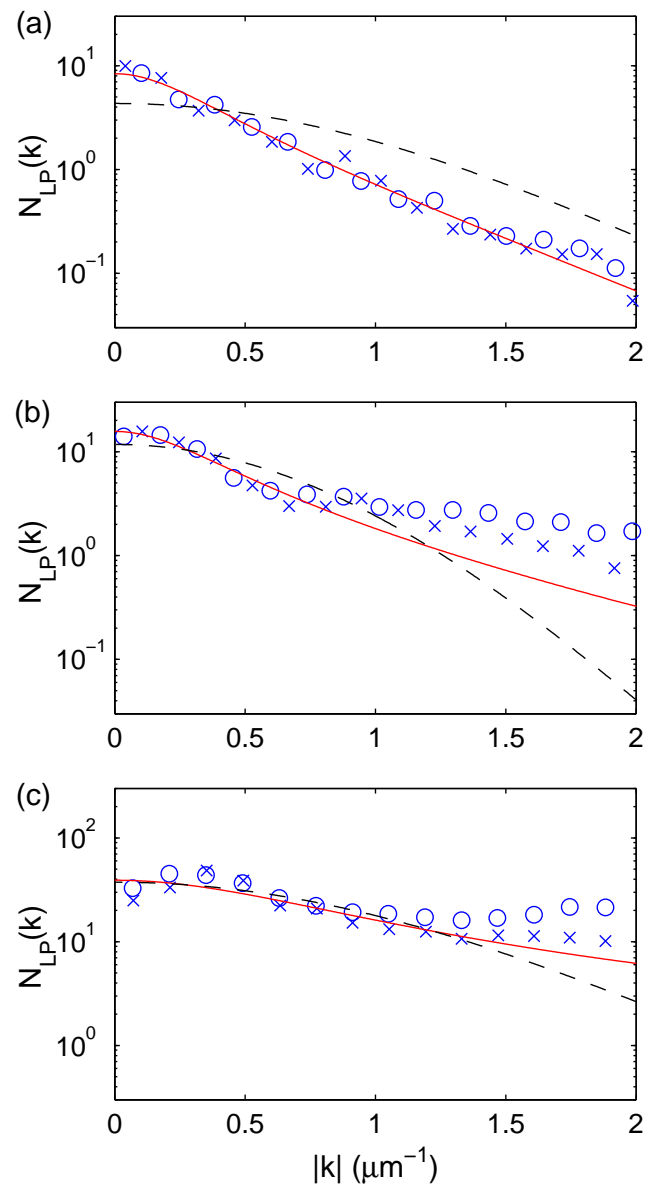


FIG. 5: Replot of Fig 2 using log-scale for y-axis. The full scales of the y-axes are: (a)  $0:03$   $[1 \cdot 10^3]$ , (b)  $0:03$   $[1 \cdot 10^3]$ , (c)  $0:3$   $[1 \cdot 10^3]$ .

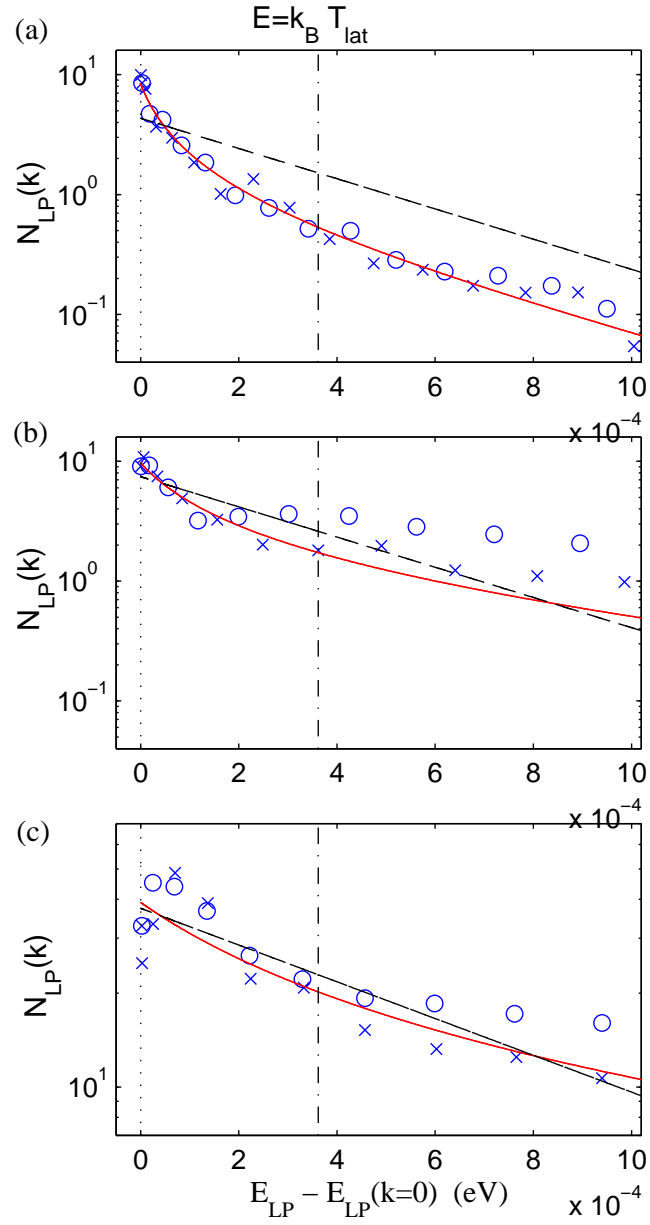


FIG. 6: Re-plot of Fig 2 using log-scale for the y-axis and  $E_{LP}(k) - E_{LP}(0)$  instead of  $k$  for the x-axis. The full scales of the y-axes are: (a) 0.04 [1 400], (b) 0.04 [1 400], (c) 7 [1 10]. The vertical dash-dot line marks  $E = k_B T_{lat} = 0.36$  m eV